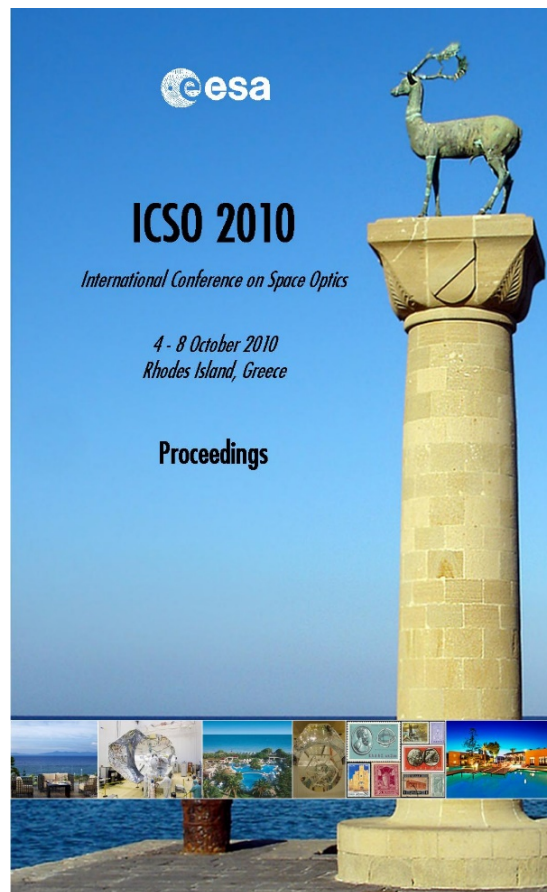


International Conference on Space Optics—ICSO 2010

Rhodes Island, Greece

4–8 October 2010

*Edited by Errico Armandillo, Bruno Cugny,
and Nikos Karafolas*



Fully programmable micro diffraction grating for VIS and near-IR spectroscopic applications

R. Lockhart, B. Timotijevic, M. Canonica, W. Noell, et al.



International Conference on Space Optics — ICSO 2010, edited by Errico Armandillo, Bruno Cugny, Nikos Karafolas, Proc. of SPIE Vol. 10565, 105656C · © 2010 ESA and CNES
CCC code: 0277-786X/17/\$18 · doi: 10.1117/12.2552745

FULLY PROGRAMMABLE MICRO DIFFRACTION GRATING FOR VIS AND NEAR-IR SPECTROSCOPIC APPLICATIONS

R. Lockhart¹; B. Timotijevic¹; M. Canonica²; W. Noell²; F. Zamkotsian³; R. P. Stanley¹; M. Tormen¹

¹CSEM SA - Centre Suisse d'Electronique et Microtechnique, Switzerland.

²EPFL- Ecole Polytechnique Federale Lausanne, Switzerland.

³LAM - Laboratoire d'Astrophysique de Marseille, France.

I. INTRODUCTION

Programmable Micro Diffraction Gratings (PMDG) are one dimensional arrays of individual mirrors, the height of which can be adjusted to produce a desired spectrum at a given angle. They can function both as spatial light modulators and as reconfigurable generators of high-resolution spectra. Fig. 1a shows the way the PMDG is actuated, while Fig. 1b presents an example of applications for PMDGs, the generation of synthetic spectra [12]. MEMS PMDGs have been used in microspectrometers, compact projection displays, optical communication systems and miniaturized external cavity lasers [1-4] because of their optical properties and compactness.

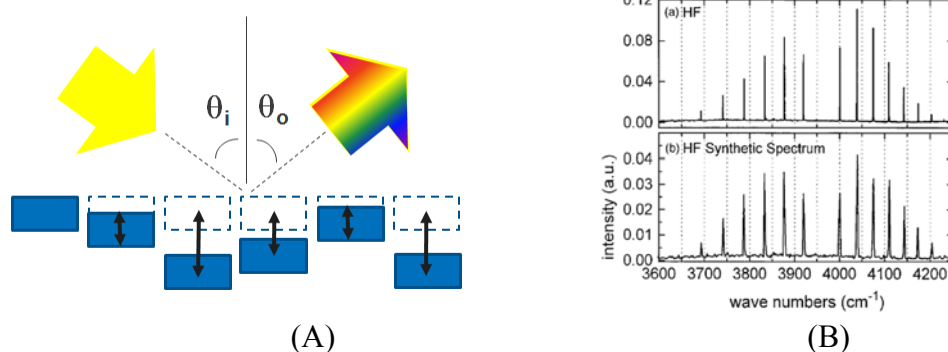


Fig. 1. A) Cross-section of actuated Programmable micro diffraction grating. B) Example of generated spectrum. (a) Spectrum (1-T) of gaseous HF. (b) Calculated synthetic spectrum from a diffractive element designed to detect HF [12].

In commercial PMDGs, only every second micro-mirror is actuated [5]. In most cases the diffraction efficiency of the device is reduced due to bending of the micro-mirrors during actuation [1, 6]. The diffraction efficiency drops by more than 50% for curvatures of $\lambda/4$. In the cases where the micro-mirror bending is kept under control, the design and fabrication have become rather complex; such an example is the multi-level PMDG by Polychromix [7].

In this work we present the design, fabrication and characterization of a Fully Programmable Micro Diffraction Grating (F-PMDG). The key design criteria were: an n -element array in which all n elements can be displaced out-of-plane independently, operations up to 2 μm in wavelength (requiring a maximum out-of-plane deflection of 1 μm), grating element length at least 700 μm , bending less than $\lambda_{\text{min}}/10$, grating filling factor > 90%, single ribbon reflectivity > 80%, actuation time < 1ms.

The F-PMDG fabrication requires only three photolithography masks.

II. DEVICE DESIGN

The principle of the proposed fully programmable micro diffraction grating (F-PMDG) is illustrated in Fig. 2: rigid micro-mirrors are connected to the center of two compliant mechanical flexures via linkage arms. The electrostatic force from an applied potential between the flexures and the underlying electrodes pulls the flexures towards the substrate. The separation of the optical micro-mirror from the mechanical flexures permits the mirrors to follow the vertical displacement of the flexures without applying a force directly to the mirror. The absence of force acting on the micro-mirror vastly reduces the degree of mirror bending during actuation.

A desired spectrum at a given diffraction angle can be produced by varying the heights of the individual mirrors. The phase shifts required for fully dispersed and non-dispersed spectral inputs are equal to π and 2π , respectively. Therefore, strokes of $\lambda_{\text{max}}/4$ or $\lambda_{\text{max}}/2$ are required for diffractive devices that work in reflection. The maximum stroke of the designed F-PMDG is 1 μm permitting full phase control and spectra generation up to $\lambda_{\text{max}}=2\mu\text{m}$.

Long and large mirrors reduce the complexity of the optics in the surrounding system and help to dissipate the energy from high intensity input sources. Because of these reasons, the micro-mirrors were designed with relatively big widths and lengths, 120 μ m and 700 μ m respectively.

On the other hand, in order to incorporate a large number of micro-mirrors (>1000), the micro-mirror width should be kept as small as possible (<50 μ m).

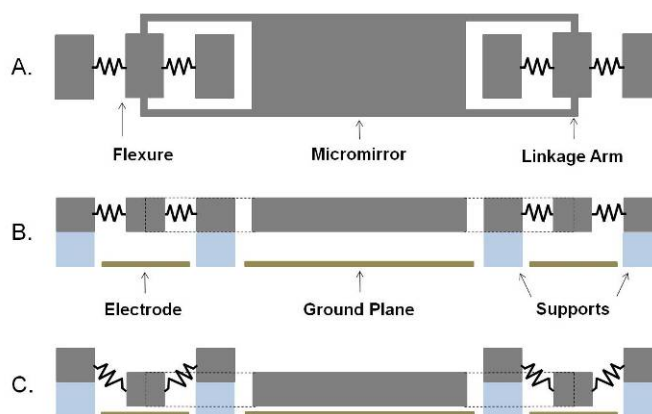


Fig. 2. 2D schematic of a single micro-mirror: a) top-down view; b) side view in the rest state and, c) side view in the actuated state. A potential applied between the flexure and the underlying electrode pulls the flexures towards the substrate causing the central micro-mirror to displace vertically.

The maximum stroke of the micro-mirrors in the F-PMDG is governed by the pull-in instability common to all parallel plate actuators. This occurs when the free-space gap between the flexures and the electrodes is reduced to $\sim 2/3$ of the initial gap [8]. The voltage at which this instability occurs is given by relation

$$V_{PI} = \sqrt{\frac{8kg_0^3}{27\varepsilon_0 A_{eff}}} \quad (1)$$

where g_0 is the initial free-space gap, ε_0 is the permittivity of free space, A_{eff} is the effective area of the electrodes, and k is the spring constant of the flexures. Equation (1) defines the upper limit of the operational voltage range for a parallel plate actuator. Thus, to ensure that the maximum operating voltage for complete actuation of the micro-mirrors is below the minimum potential leading to electrostatic breakdown in air, the flexures must be designed with the appropriate spring constant.

The F-PMDG was designed using serpentine flexures (Fig. 3). Due to the geometry of the serpentine flexure, the spring constant varies approximately linearly with the thickness of the structure compared to the well-known cubic relation, valid for simple clamped-clamped rectangular flexures. This enables compliant flexures to be fabricated alongside the micro-mirrors on the same optomechanical device layer without compromising the stiffness of the mirrors.

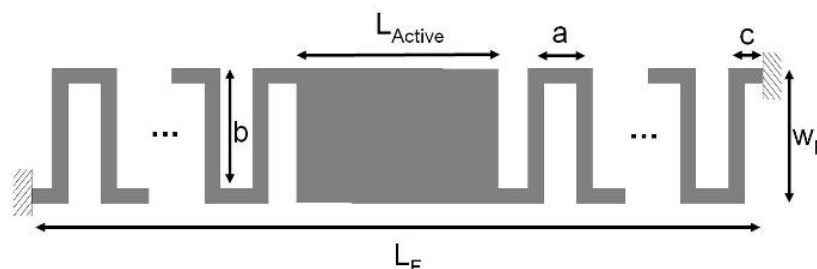


Fig. 3. Schematic of a serpentine flexure.

For 120 μ m wide mirrors with a critical dimension (CD) of 5 μ m, where a and b are set to 10 μ m and 100 μ m respectively, whereas the number of meanders (n) is set to 4, the spring constant of the flexures of 18N/m can be achieved. Consequently, for a total flexure length (L_F) equal to 300 μ m, the micro-mirror can be fully actuated with voltages as low as 30V with the out-of-plane resonant frequency as high as 14 kHz.

III. FABRICATION

Fabrication of the F-PMDG follows a process flow incorporating only three photolithography masks.

Steps (a) through (d) are shown in the simplified process flow presented in Fig. 4. Processing begins with a clean Pyrex 7740 glass wafer. An aluminum hard mask is patterned on the surface and used to etch cavities and support posts into the glass wafer by anisotropic deep reactive ion etching (DRIE) (Fig. 4a). The depth of the cavities determines the maximum stroke of the mirrors along with the required actuation voltage. 3 μ m deep cavities were etched into glass wafers to permit the micro-mirrors 1 μ m of vertical travel. The aluminum mask is then removed and a thick high-aspect ratio photoresist is patterned on the wafers to define the bond pads and the electrodes using a lift-off procedure. The resist is hard-baked to improve the adhesion with the substrate and dipped into buffered hydrofluoric acid (BHF) for several minutes to slightly underetch the Pyrex beneath the photoresist in order to ease the lift-off in the next step. Cr/Pt metal layers are then deposited on the glass wafer by e-beam evaporation, followed by the electrode patterning and removal of the photoresist (lift-off) (Fig. 4b).

The 4 μ m thick device layer of an unpatterned silicon-on-insulator (SOI) wafer is anodically bonded to the patterned surface of the Pyrex wafer (Fig. 4c). The handle layer of the SOI wafer is then dissolved in potassium hydroxide (KOH). Etching of the handle layer is stopped before arriving at the insulating oxide layer. The thermally grown oxide does act as an etch stop for the Si handle removal in KOH; however, small pinholes in the thin oxide layer can allow small amounts of KOH to breach this masking layer causing damage to the silicon device layer. Dokmeki *et al.* have shown that the device yield can be improved by removing the wafer stack from the KOH bath before reaching the oxide and removing the remaining handle layer using RIE [10]. The oxide layer is also removed by RIE before performing the final photolithography step to pattern the micro-mirrors and flexures into the SCS device layer (Fig. 4d). The 4 μ m thick silicon layer is anisotropically etched by DRIE. At this point, the micro-mirrors are fully released. Thus, the remaining photoresist mask is removed by oxygen plasma.

Fig. 5a is a 4-beam grating image from an optical microscope, Fig. 5b is a 64-beam grating image from the Scanning Electron Microscope (SEM).

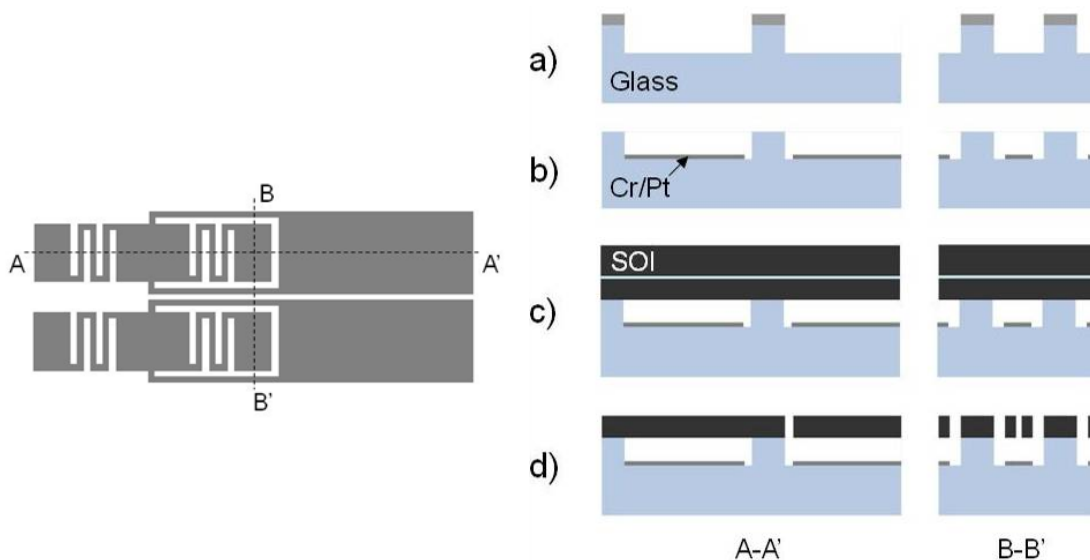


Fig. 4. Simplified process flow for a F-PMDG. (Left) The top-view of 2 half-micro-mirrors. The orthogonal dashed lines indicate the cross-sections at which the process flow is explained on the right. (Right) (a) Patterned metal mask on a Pyrex glass wafer is used to etch cavities and support posts; (b) Cr/Pt electrodes patterning by lift-off; (c) anodic bonding of SOI wafer; (f) patterning of the device layer & release of the mirrors.

Low stress devices were bonded at 350°C in atmospheric pressure with 800V applied across the stack. Using these conditions, the residual stress in the SCS layer was reduced to ~2MPa of tensile stress at the interface. As a result, peak-to-valley variations of <10nm have been measured along fabricated micro-mirrors. This is equivalent to a radius of curvature (ROC) equal to 8m.

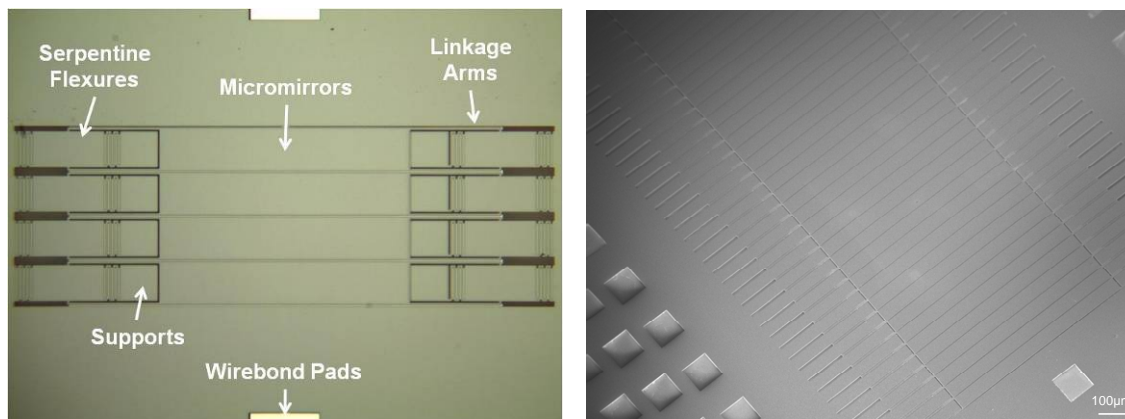


Fig. 5. a) Optical image of a F-PMDG with 4 micro-mirrors. The mirrors are $120\mu\text{m}$ wide and $700\mu\text{m}$ long with $300\mu\text{m}$ long serpentine flexures situated on either side. The wirebond pads on both sides of the grating are used as connection points to the electrodes lying beneath the flexures. b) An SEM micrograph of a F-PMDG with 64 micro-mirrors, $50\mu\text{m}$ wide, and $700\mu\text{m}$ long.

IV. CHARACTERIZATION

The gratings were diced and wirebonded for electromechanical and optical characterization. Vertical displacement of the micro-mirrors versus applied voltage was measured using a white light interferometer.

It was shown that mirrors with serpentine flexures can be vertically displaced up to $1\mu\text{m}$ with $<30\text{V}$.

Fig. 6a represents a comparison of Finite Element Method (FEM) simulated values with the experimentally measured displacement of several micro-mirrors versus applied voltage.

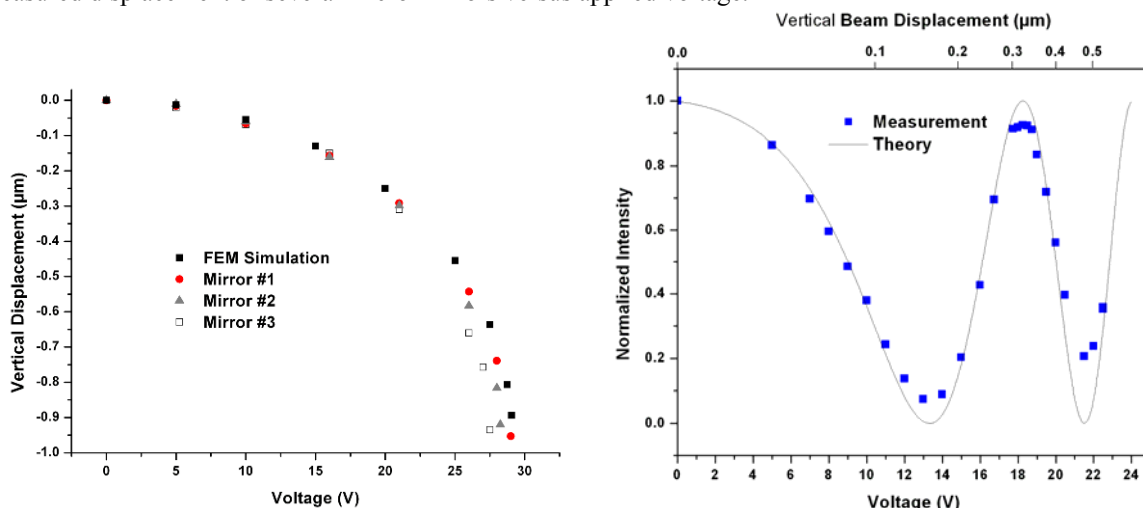


Fig. 6. a) Measured vertical displacement versus actuation voltage for 3 micro-mirrors and comparison to FEM simulated data. A noticeable variation between the mirrors at large displacements is due to the post-fabrication variation in the flexures. b) The intensity in the zeroth order for a monochromatic light source ($\lambda=632.8\text{nm}$) reflecting off the F-PMDG while varying the vertical displacement of every second micro-mirror. At $\lambda/4$ the intensity drops below 10% recovering to $>90\%$ at $\lambda/2$.

The optical performance of the device is demonstrated in Fig. 6b where the intensity of the zeroth order was recorded while displacing every second beam by an amount d . The measured intensities closely follow that of the simulated theoretical response. Moreover, they demonstrate the high efficiency and contrast ratio possible with the presented device as a result of rigid optical beams.

A vertical position of a mirror for several actuation voltages in a range $0 - 29\text{V}$ is presented in Fig. 7a. This demonstrates pure piston motion of the mirror in a range between 0 and $1\mu\text{m}$.

Flatness of the micro-mirrors during actuation has also been verified using the white light interferometer. The measured height difference between the center and the edges of the $700\mu\text{m}$ long mirror is less than 10nm . This is equivalent to $\lambda/60$ for visible light or a radius of curvature of 7m (Fig. 7b).

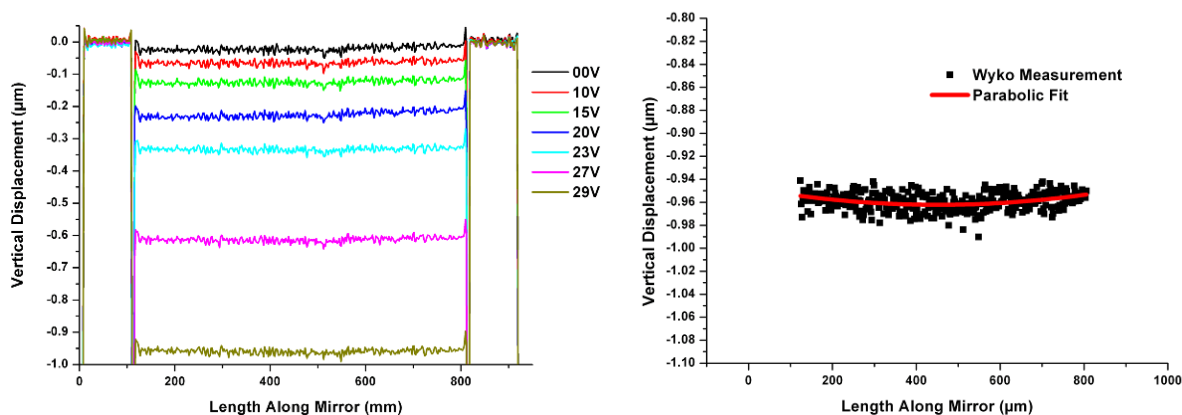


Fig. 7. a) Surface profile of a single micro-mirror for applied voltages between 0-29V. The mirror undergoes pure piston motion up to $1\mu\text{m}$ while remaining optically flat. b) Parabolic fit of the surface profile of a single mirror that has been vertically deflected by $1\mu\text{m}$. The radius of curvature is 7m.

V. CONCLUSIONS

We have demonstrated a fully programmable micro diffraction grating (F-PMDG) in which the micro-mirrors of an n -element array can be individually deflected out of plane. The actuation mechanism has been designed to allow pure piston motion of the mirrors – eliminating detrimental bending. Flexures incorporating serpentine structures have been used to reduce the required actuation voltage to $<30\text{V}$ while maintaining an optical flatness better than $\lambda/40\mu\text{m}$ for visible light at vertical displacements of $1\mu\text{m}$. F-PMDG arrays of $4 - 120\mu\text{m}$ wide and $700\mu\text{m}$ long micro-mirrors have been fabricated and characterized to test the proposed concept.

Based on these results a new generation of F-PMDGs is currently being fabricated. Arrays with up to 1024 individually controllable micro-mirrors are being produced to be used as programmable diffractive devices capable of generating high-resolution spectra.

REFERENCES

- [1] O. Solgaard, F.S.A. Sandejas, and D.M. Bloom. Deformable Grating Optical Modulator. *Opt. Lett.*, 17:668-690, 1992.
- [2] G. B. Hocker, D. Youngner, E. Deutsch, A. Volpicelli, S. Senturia, M. Butler, M. Sinclair, T. Plowman, and A. J. Ricco, "The Polychromator: A MEMS Diffraction Grating for Synthetic Spectra," Solid-State Sensor and Actuator Workshop, Hilton Head Island, SC, June 4-8, 2000, pp. 89-91.
- [3] S.D. Senturia, D.R. Day, M.A. Butler, M.C. Smith, Programmable diffraction gratings and their uses in displays, spectroscopy, and communications, *J. Microlith., Microfab., Microsyst.* 4(4) 2005.
- [4] R. Lockhart, M. Tormen, P. Niedermann, T. Overstolz, A. Hoogerwerf, R.P. Stanley. High-efficiency MEMS tuneable gratings for external cavity lasers and microspectrometer, *IEEE/LEOS Int. Conf. Optical MEMS and Nanophotonics*, (2008) pp. 33-4.
- [5] D. Yan, S. Madison, B. Xu, and J. Castracane. Analysis and testing of an optical add/drop multiplexer based on MEMS micro-actuators, *Proc. SPIE*, Vol. 4907, 1 (2002)
- [6] D.M. Burns, V.M. Bright, Development of microelectromechanical variable blaze gratings, *Sensors and Actuators A* 64 (1998)
- [7] E. R. Deutch. Achieving Large Stable Vertical Displacement in Surfaced Micromachined MEMS. PhD thesis, MIT, Cambridge, MA, 2002.
- [8] S. D. Senturia. *Microsystem Design*. Kluwer Academic Publishers, Boston, 2003.
- [9] G.K. Fedder. Simulation of Micromechanical Systems. PhD thesis, UC Berkeley, 1994.
- [10] M.R. Dokmeci, A. Pareek, S. Bakshi, M. Waelti, C.D. Fung, K.H. Heng, C.H. Masterangle, Two-Axis Single-Crystal Silicon Micromirror Arrays, *J. Micromechanical Systems* 13:1006-1017, 2004.
- [11] A. Cozma and B. Puers. Characterization of the electrostatic bonding of silicon and pyrex glass. *J. Micromech. Microeng.*, 5:98-102, 1998.
- [12] M. B. Sinclair, M. A. Butler, A. J. Ricco, and S. D. Senturia, "Synthetic spectra: a tool for correlation spectroscopy," *Appl. Opt.* 36, 3342-3348 (1997).